

DEFEND: A Large-scale 1M Dataset and Foundation Model for Tobacco Addiction Prevention

Naga VS Raviteja Chappa¹, Matthew Shepard¹, Connor McCurtain¹, Charlotte McCormick²,
Page Daniel Dobbs², Khoa Luu¹

¹Dept. of EECS, University of Arkansas

²Center for Public Health and Technology, University of Arkansas

{nchappa, mjs042, crm063, cem044, pdobbs, khoaluu}@uark.edu

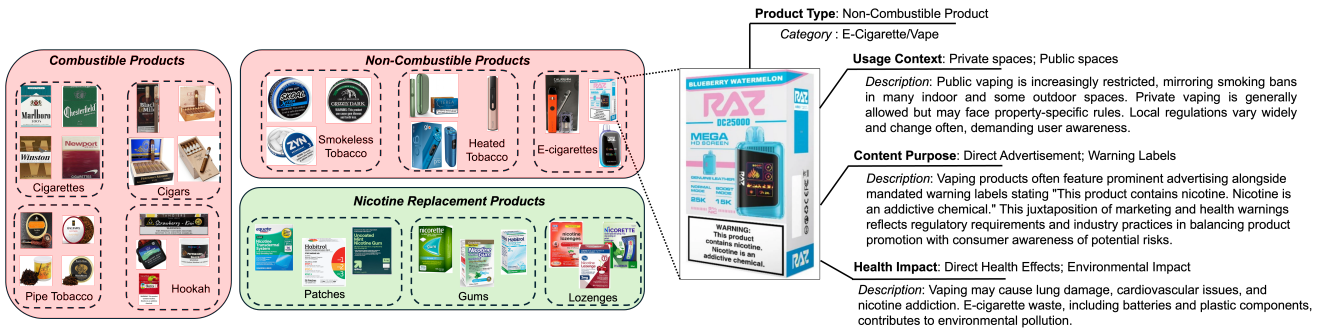


Figure 1. Examples of Our Tobacco-1M Dataset for Tobacco Product Understanding. The left section displays visual samples from the major product categories, including **Combustible Products**, **Non-Combustible Products**, and **Nicotine Replacement Products**. The right section demonstrates a hierarchical annotation example of an E-cigarette product with detailed categorical descriptions. **Note:** This dataset is *not intended* for the promotion of any tobacco products.

Abstract

While tobacco advertising innovates at unprecedented speed, traditional surveillance methods remain frozen in time, especially in the context of social media. The lack of large-scale, comprehensive datasets and sophisticated monitoring systems has created a widening gap between industry advancement and public health oversight. This paper addresses this critical challenge by introducing *Tobacco-1M*, a comprehensive dataset of one million tobacco product images with hierarchical labels spanning 75 product categories, and *DEFEND*, a novel foundation model for tobacco product understanding. Our approach integrates a Feature Enhancement Module for rich multi-modal representation learning, a Local-Global Visual Coherence mechanism for detailed feature discrimination, and an Enhanced Image-Text Alignment strategy for precise product characterization. Experimental results demonstrate *DEFEND*'s superior performance, achieving 83.1% accuracy in product classification and 73.8% in visual question-answering tasks, outperforming existing methods by signifi-

cant margins. Moreover, the model exhibits robust zero-shot learning capabilities with 45.6% accuracy on novel product categories. This work provides regulatory bodies and public health researchers with powerful tools for monitoring emerging tobacco products and marketing strategies, potentially revolutionizing approaches to tobacco control and public health surveillance.

1. Introduction

Tobacco addiction persists as a critical public health challenge, with particularly severe implications for youth and young adults. The tobacco industry's rapid innovation in product development, including e-cigarettes and novel nicotine delivery systems, has consistently outpaced regulatory efforts and traditional monitoring methods. This dynamic landscape creates significant obstacles for public health officials, researchers, and policymakers in effectively addressing tobacco use and its far-reaching health impacts. Accurate detection and classification of tobacco products serve as a critical foundation for addiction prevention by enabling

regulatory bodies to identify new products, enforce marketing restrictions, and develop targeted intervention strategies for vulnerable populations.

Existing tobacco product detection and classification methods have been constrained by limited datasets, often focusing on a narrow range of product types. Recent studies, such as Murthy *et al.* [33], Vassey *et al.* [40], and the PHAD dataset [8], have made progress by expanding the number of product types examined. However, while valuable, these efforts still fall short of capturing the full spectrum of tobacco products in today’s diverse market, thus limiting their utility in comprehensive tobacco control efforts.

The advent of foundation models in artificial intelligence offers a promising avenue for developing more robust and adaptable tobacco product monitoring systems. Recent advancements have demonstrated the power of these models, pre-trained on large-scale datasets, in revolutionizing vision tasks and generalizing well to various downstream applications [3, 11, 17, 19, 37]. They excel at capturing both general and specific properties of visual data, making them potentially valuable tools for tobacco product analysis.

However, the development of effective foundation models for tobacco product monitoring faces a significant hurdle: the lack of a sufficiently large and diverse dataset. Current tobacco-related datasets, as evidenced by our comparative analysis (Table 1), are limited in scale and scope. This limitation mirrors challenges observed in other domains, such as insect recognition [43], where the diversity and complexity of the subject matter demand datasets of unprecedented scale and detail.

Contributions of this Work: To advance tobacco product monitoring and analysis, we introduce **Tobacco-1M**, a comprehensive tobacco product dataset, and **Distillation-enabled Enhanced Feature learning for tobacco ENforcement and Discernment (DEFEND)**, a novel foundation model for tobacco product understanding. First, we present Tobacco-1M, comprising one million images with hierarchical labels spanning from broad categories (e.g., Combustible, Non-Combustible) to specific types (e.g., Cigarettes, E-cigarettes), each annotated with detailed descriptions of features, usage context, and health impacts (refer to Fig. 1 for the dataset sample). This dataset is relatively 140 times larger than prior work [40]. Second, we introduce a self-supervised learning approach with a Feature Enhancement module that captures nuanced correlations between visual and textual features. Third, we propose a Local-Global Visual Coherence loss that ensures consistency between fine-grained and holistic product representations. Fourth, we implement an Enhanced Image-Text Alignment mechanism with specialized contrastive loss for precise feature-description mapping. Finally, through extensive experiments on product classification,

marketing strategy detection, and health impact assessment tasks, we demonstrate significant performance improvements over existing tobacco control and public health research methods.

2. Related Works

Recent advancements in video analysis [4, 5, 28, 35, 39, 42, 46, 48–51] have predominantly employed traditional deep learning algorithms, but the absence of language comprehension limits their efficacy. Recognizing this gap, there is a shift towards integrating text modalities [7, 9] to enhance understanding capabilities. It underscores the need to evolve existing algorithms, advocating for joint training with Large Language Models (LLMs) [25] to achieve superior performance and nuanced comprehension.

Foundation Models and Multimodal Learning. Recent foundation model research [10, 30, 44] has advanced multimodal approaches, integrating diverse data sources for richer representation learning. These models have demonstrated particular success in hierarchical learning [2, 31], enabling classification across both broad and fine-grained categories. Transfer learning capabilities [15, 21] have further extended their utility, allowing models trained on one domain to generalize to related tasks. For instance, Luis *et al.* [15] successfully applied transfer learning to connect training across DNA, RNA, and protein sequences, demonstrating the potential for cross-domain knowledge transfer.

Tobacco Content Analysis in Social Media. Recent studies [6, 23, 32] have employed machine learning techniques to analyze e-cigarette content and promotion strategies on platforms like YouTube, focusing on how user profiles influence content engagement. Prior work [40] developed computer vision models using Instagram data (6,999 images) labeled for e-cigarette-related objects, while Murthy *et al.* [33] extended this to TikTok using YOLOv7 [41] for detecting vaping devices and related content in 826 annotated images.

AI Applications in Tobacco Research. Machine learning has been increasingly applied to broader tobacco research domains. Studies have utilized regression tree models for analyzing global tobacco survey data [22], identifying factors contributing to adolescent tobacco use. Other research has focused on smoking cessation [36], using machine learning to predict and analyze relapse patterns through app-based data collection. Recent work [24] has demonstrated the potential of deep learning in detecting covert tobacco advertisements through integrated multimodal analysis of text and images.

Large-scale Dataset Development. While existing datasets have contributed to tobacco content analysis, they remain limited in scale and scope. Current public datasets range from 826 images [33] to 6,999 images [40], focusing primarily on specific product categories or platforms.

3.3. Dataset Statistics

Figure 2 (left) illustrates the distribution of auxiliary categorization levels in Tobacco-1M, with Product Type dominating. It also shows subcategory distributions, notably a balanced representation of health concerns within the Health Impact Depiction category. Figure 2 (center) breaks down Product Types and brands, revealing combustible products, especially cigarettes, as the majority. Brand distribution within each Product Type is comprehensive. The dataset balances real-world product prevalence with diversity, enabling robust AI model development across the tobacco product spectrum.

3.4. Significance and Potential Applications

Tobacco-1M’s comprehensive categorization and diverse coverage facilitate the development of generalizable AI models for tobacco product detection, classification, and trend analysis. It supports research on product evolution, health impacts, and regulatory compliance across jurisdictions (refer to Sec. G of Supp.). This dataset aims to accelerate AI-driven tobacco monitoring research, contributing to effective control policies. Tobacco-1M serves as a vital resource for researchers, policymakers, and health professionals in reducing tobacco-related disease burden globally.

4. Methodology

4.1. Limitations in Prior Training Approaches

A critical challenge in tobacco product understanding is the accurate representation and interpretation of subtle product features that distinguish different categories and variants. While CLIP [37] demonstrates strong performance in general visual-language tasks, it struggles to capture fine-grained product attributes and regulatory elements crucial for tobacco product analysis. Similarly, vision-language models like CoCa [47] process images holistically, often missing the detailed textural and structural characteristics that differentiate tobacco products.

Current approaches using masked image modeling [18] focus primarily on broad feature reconstruction without explicitly addressing the nuanced visual elements of tobacco products, which is visualized in Fig. 3. While hierarchical vision transformers [14] attempt to capture multi-scale features, they lack mechanisms to combine local product details with global contextual understanding effectively. Furthermore, existing contrastive learning methods [45] emphasize general semantic alignment between images and text, but fail to capture the specialized relationships between tobacco product attributes and their technical descriptions.

To overcome these challenges, we introduce DEFEND (as illustrated in Fig. 4), a novel framework that synergizes global product understanding with local feature discrimination through an innovative teacher-student architecture. Our

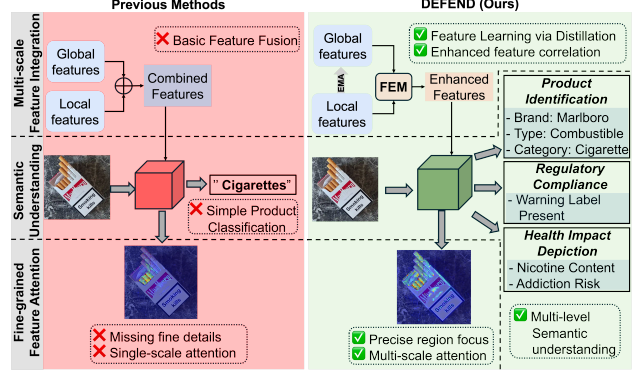


Figure 3. **Comparisons of Previous Methods.** Prior works [14, 18, 45, 47] demonstrate significant limitations in tobacco product analysis: naive feature fusion fails to capture nuanced product characteristics due to oversimplified integration, basic classification architecture overlooks critical regulatory elements. DEFEND overcomes these limitations through Feature Enhancement Module (FEM), enabling precise feature correlation across scales, that distinguishes critical regulatory elements and health impact indicators through targeted region focus and multi-scale attention mechanisms. **Best viewed with zoom in and color.**

approach not only enhances the model’s ability to capture subtle product characteristics but also maintains semantic consistency across different scales of visual analysis.

4.2. Input Modeling

Given an input image $I \in \mathbb{R}^{H \times W \times 3}$, we process it into two complementary representations, including a global view G and a set of local patches $P = \{p_i\}_{i=1}^{N_P}$. The number of patches is determined by $N_P = HW/s_p^2$, where $s_p \times s_p$ is the patch resolution. To enhance feature discrimination, we employ an adaptive sampling strategy as in $P_s = \Psi(P, \lambda) \subset P$, where Ψ is our adaptive sampling function (detailed in Sec. C.1 of Supp.) that selects patches based on saliency parameter λ , focusing on regions with distinctive product characteristics. This dual representation enables our model to simultaneously capture global context and local details crucial for tobacco product analysis.

4.3. Teacher-Student Architecture

Our framework employs a teacher-student architecture where knowledge is distilled from the student to the teacher through Exponential Moving Average (EMA) updates while maintaining a stable global view of tobacco products. This design helps capture broad product categories and subtle distinguishing features like warning labels and brand elements.

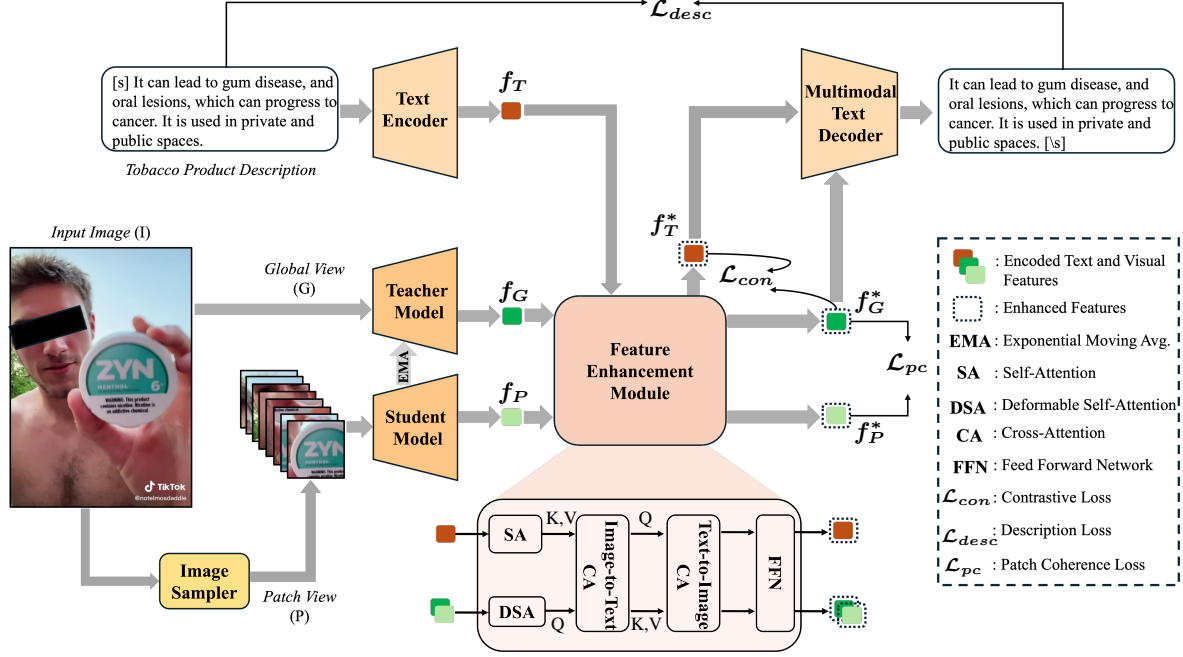


Figure 4. **Overview of our proposed DEFEND Framework.** We employ a dual-stream design where text input is processed through a Text Encoder while image input follows two parallel paths through a Teacher-Student architecture. The Feature Enhancement Module enhances these multimodal features, which are then used to train the model with multiple objectives, including contrastive, description, and patch coherence losses, to generate comprehensive multimodal representations.

4.3.1 Teacher Model - The Global Encoder

The teacher model E_{global} serves as a stable global feature extractor. It processes the entire image to establish a holistic understanding, as in Eqn. (1).

$$f_G = E_{global}(G), \quad f_G \in \mathbb{R}^{1 \times D} \quad (1)$$

where D is the feature dimension. Knowledge is distilled from the student to the teacher through EMA updates of the network parameters: $\theta_t^{(k)} = \alpha \theta_t^{(k-1)} + (1 - \alpha) \theta_s^{(k)}$ where $\theta_t^{(k)}$ and $\theta_s^{(k)}$ are the teacher and student parameters at iteration k respectively, and $\alpha \in [0, 1]$ is the EMA decay rate (typically set to 0.999).

4.3.2 Student Model - The Patch Encoder

The student model E_{patch} learns to extract discriminative local features under the teacher’s guidance. For each sampled patch $p_i \in P_s$, it generates features encouraged to align with the teacher’s global understanding, as in Eqn. (2).

$$\mathbf{X}_s = \text{concat}[\mathbf{x}_i]_{i=1}^{N_{P_s}} \in \mathbb{R}^{N_{P_s} \times D}, \quad \mathbf{x}_i = \alpha_p(p_i) + \mathbf{e}_p(i) \quad (2)$$

where α_p is a patch projection function and \mathbf{e}_p is a learnable position embedding that maintains spatial relationships between patches. The student processes these patches through

L_e transformer blocks as follows,

$$\mathbf{X}'_l = \mathbf{X}_{l-1} + \text{MSA}(\text{LN}(\mathbf{X}_{l-1})) \quad (3)$$

$$\mathbf{X}_l = \mathbf{X}'_l + \text{FFN}(\text{LN}(\mathbf{X}'_l)) \quad (4)$$

$$\mathbf{X}_0 = \mathbf{X}_s, \quad 1 \leq l \leq L_e \quad (5)$$

where MSA denotes multi-head self-attention, LN is layer normalization, and FFN represents a feed-forward network. The final patch-level features are obtained as in Eqn. (6).

$$f_P = E_{patch}(\mathbf{X}_s), \quad f_P \in \mathbb{R}^{N_{P_s} \times D} \quad (6)$$

Through this EMA-based knowledge transfer, the student learns to extract local features while the teacher maintains a stable global view.

4.4. Text Encoder

The text encoder processes input descriptions to create representations that can effectively align with our visual features. Given a text description $T = \{t_i\}_{i=1}^{N_T}$, where N_T is the number of tokens, we employ BERT [12] as our text encoder E_{text} to generate contextual representations as follows,

$$f_T = E_{\text{text}}(T), \quad f_T \in \mathbb{R}^{N_T \times D} \quad (7)$$

$$\mathbf{H}_l = \text{MSA}(\text{LN}(f_T^{l-1})) + f_T^{l-1} \quad (8)$$

$$f_T^l = \text{FFN}(\text{LN}(\mathbf{H}_l)) + \mathbf{H}_l, \quad l = 1, \dots, L_t \quad (9)$$

where L_t is the number of transformer layers, MSA denotes multi-head self-attention, LN is layer normalization, FFN is a feed-forward network, and f_T^0 represents the initial token embeddings.

4.5. Feature Enhancement Module

The Feature Enhancement Module (FEM) enriches both visual and textual representations through a unified multi-stage attention mechanism. Given global features $\mathbf{f}_G \in \mathbb{R}^{1 \times D}$ from the teacher and patch features $\mathbf{f}_P \in \mathbb{R}^{N_{P_s} \times D}$ from the student, we process these representations through intra-modal and cross-modal attention stages.

The feature enhancement process begins with modality-specific self-attention as follows,

$$\hat{f}_T = A_T(\mathbf{f}_T, \mathbf{f}_T, \mathbf{f}_T), \quad (10)$$

$$\hat{f}_V = A_V(\mathbf{f}_V, \mathbf{f}_V, \mathbf{f}_V), \quad V \in \{G, P\} \quad (11)$$

where A_T and A_V are modality-specific self-attention mechanisms. The cross-modal attention and refinement then proceed as follows,

$$\mathbf{f}_T^* = F_T(A_{TV}(\hat{f}_T, \hat{f}_V, \hat{f}_V)) \quad (12)$$

$$\mathbf{f}_V^* = F_V(A_{VT}(\hat{f}_V, \hat{f}_T, \hat{f}_T)), \quad V \in \{G, P\} \quad (13)$$

where A_{TV} and A_{VT} are cross-modal attention operations, and F_T and F_V are feed-forward networks for final feature refinement. Each attention mechanism follows the scaled dot-product attention: $\text{Attention}(\mathbf{Q}, \mathbf{K}, \mathbf{V}) = \text{softmax}(\frac{\mathbf{Q}\mathbf{K}^T}{\sqrt{d}})\mathbf{V}$, where \mathbf{Q} , \mathbf{K} , and \mathbf{V} represent query, key, and value matrices respectively, and d is the feature dimension.

4.6. Enhanced Image-Text Alignment

To further improve the alignment between visual and textual representations, inspired by recent advances in vision-language modeling [37, 47], we employ a contrastive learning strategy. While these works demonstrate the effectiveness of contrastive learning for general image-text alignment, we adapt this approach specifically for tobacco product understanding by leveraging our enriched multimodal features from FEM.

The contrastive loss \mathcal{L}_{cont} encourages semantic alignment between matched image-text pairs while distinguishing unrelated pairs as $\mathcal{L}_{cont} = -\log \frac{\exp(s(\mathbf{f}_T^*, \mathbf{f}_G^*)/\tau)}{\sum_k \exp(s(\mathbf{f}_T^*, \mathbf{f}_{G_k}^*)/\tau)}$, where $s(\cdot, \cdot)$ denotes cosine similarity, τ is a temperature parameter, and $\mathbf{f}_{G_k}^*$ represents global features from other samples in the batch. By applying this loss to our enhanced features \mathbf{f}_T^* and \mathbf{f}_G^* , we leverage the rich representations learned through our FEM to create more precise alignments between product images and their technical descriptions.

4.7. Local-Global Visual Coherence

Maintaining consistency between fine-grained details and overall product characteristics in tobacco product analysis is essential for accurate classification and attribute detection. Local features must align with the global context while preserving discriminative details specific to product categories and variants. To achieve this balance, we introduce a patch coherence mechanism.

The patch coherence loss \mathcal{L}_{pc} ensures alignment between local and global representations as $\mathcal{L}_{pc} = \|\mathbf{f}_G^* - \text{AvgPool}(\mathbf{f}_P^*)\|_2^2$. This loss term ensures that local patch representations contribute coherently to the global product understanding while maintaining their distinctive characteristics.

4.8. Multimodal Image Description Decoder

While contrastive learning establishes broad semantic alignments, but precise description of tobacco products requires capturing intricate product attributes, regulatory elements, and interrelationships. Our decoder architecture addresses this by incorporating enhanced visual and textual representations in a structured generation process.

The multimodal description generation process and training objective are formalized as follows:

$$h_j = \text{DecoderLayer}([y_{<j}; \mathbf{f}_T^*; \mathbf{f}_G^*]) \quad (14)$$

$$p(y_j|y_{<j}) = \text{softmax}(\mathbf{W}_o h_j + b_o) \quad (15)$$

$$\mathcal{L}_{desc} = -\frac{1}{N} \sum_{i=1}^N \sum_{j=1}^{M_i} \log p(y_{ij}|y_{i,<j}, \mathbf{f}_T^*, \mathbf{f}_G^*) \quad (16)$$

where h_j is the decoder hidden state, \mathbf{W}_o and b_o are learnable parameters, N is the batch size, and M_i is the length of the i -th description. Please refer to Sec. B of Supp. for a detailed Inference procedure.

5. Experimental Results

5.1. Implementation Details

Datasets. We conduct our main experiments on the PHAD dataset [8], which contains 5,730 videos sampled at 24 frames per second following their experiments across eight categories. For pre-training, we utilize our newly collected Tobacco-1M dataset, comprising 1M high-resolution tobacco product images across 75 categories: combustible products (450K images), non-combustible products (200K images), and nicotine replacement products (50K images). Each image is annotated with comprehensive metadata, including product type, brand information, and health warnings. We use 700K images for training, reserving 150K for VQA task evaluation and 150K as a testing set.

Model Configurations. Our framework adopts ViT-B/16 [13] as the backbone, processing 224×224 images

with a 16×16 patch size. The model integrates an adaptive sampling mechanism ($\lambda = 0.3$) that prioritizes regions with product-distinctive features (e.g., warning labels, brand logos). For text processing, we leverage BERT [12] as our encoder and extend it with cross-attention layers for visual-textual fusion. Training proceeds in three phases on 4×A100 GPUs: warm-up (20 epochs), main training (200 epochs), and fine-tuning (80 epochs), using AdamW [26] with 1e-3 learning rate and cosine decay [27]. Please refer to Sec. C of the Supp. for comprehensive implementation details, including hyperparameter selection, data augmentation strategies, and training procedures.

Metrics. We evaluated our model using standard classification metrics: accuracy, precision, recall, and F1-score. For the visual question answering (VQA) task, we used accuracy and F1-score. Zero-shot performance was assessed using top-1 and top-5 accuracy on unseen classes.

5.2. Ablation Studies

Our comprehensive ablation study, presented in Table 2, reveals the individual and combined effects of various components in our Tobacco Foundation Model on the Tobacco-1M Classification task. Please refer to Sec. D of the Supp. for more ablation studies.

Table 2. Ablation study results on the Tobacco-1M dataset. Here, Acc.: Accuracy, FEM: Feature Enhancement Module, \mathcal{L}_{pc} : Patch Coherence Loss, \mathcal{L}_{con} : Contrastive Loss, and \mathcal{L}_{desc} : Description Loss.

Backbone	FEM	\mathcal{L}_{pc}	\mathcal{L}_{con}	\mathcal{L}_{desc}	Acc.@1 (%)	Acc.@5 (%)
ViT-small/16	✓				71.2	76.5
	✓	✓			72.4	77.3
	✓	✓	✓		73.5	78.2
	✓	✓	✓	✓	74.2	79.1
ViT-base/16	✓				73.8	78.6
	✓	✓			75.1	79.8
	✓	✓	✓		77.1	81.9
	✓	✓	✓	✓	78.3	83.1
ViT-large/16	✓				73.2	78.1
	✓	✓			74.5	79.3
	✓	✓	✓		76.2	81.1
	✓	✓	✓	✓	77.4	82.3

Note: FEM Only experiments uses basic cross-entropy loss.

Effectiveness of Backbone Networks. The study encompasses three Vision Transformer variants: ViT-small/16, ViT-base/16, and ViT-large/16. Our findings indicate that the ViT-base/16 architecture achieves the best performance, with a peak Top-1 accuracy of 78.3%. This represents a substantial improvement over both the ViT-small/16 (74.2%) and ViT-large/16 (77.4%) models, suggesting that this architecture provides an optimal balance between model capacity and efficiency in capturing the nuanced features of

tobacco products.

Effectiveness of FEM. The Feature Enhancement Module (FEM) emerges as a cornerstone of our model’s success. Its integration yields significant performance boosts across all architectures, establishing strong baseline accuracies of 71.2%, 73.8%, and 73.2% for small, base, and large models respectively. These results highlight the crucial role of FEM in extracting and refining relevant features from tobacco product images with the help of textual descriptions.

Effectiveness of Enhanced Image-Text Contrastive Loss. The incorporation of image-text contrastive loss proves highly beneficial, driving accuracy improvements of 1.1%, 2.0%, and 1.7% for small, base, and large models, respectively. This consistent performance gain across architectures demonstrates the effectiveness of aligning visual and textual representations, enabling the model to better differentiate between visually similar tobacco products.

Effectiveness of Description Loss. Our analysis reveals that the Description Loss component further refines the model’s capabilities. It yields additional accuracy improvements of 0.7%, 1.2%, and 1.2% across the three model sizes. These gains suggest enhanced alignment between visual features and product descriptions, contributing to more precise classification, particularly for products with subtle distinctions.

Effectiveness of Patch Coherence Loss. The Patch Coherence Loss demonstrates its value by consistently enhancing model performance. It improves Top-1 accuracy by 1.2%, 1.3%, and 1.3% for small, base, and large models, respectively. These improvements indicate that promoting coherence among patch representations strengthens the model’s grasp of spatial relationships within tobacco product images, leading to more robust classification outcomes.

5.3. Comparison with State-of-the-Art Methods

Tobacco Product Classification Task. We evaluated DEFEND on the PHAD dataset by fine-tuning only the linear classification layer. Our model outperformed ImageNet1K-pretrained architectures by up to 5.8%, highlighting the importance of domain-specific pretraining, as shown in Table 3. It also surpassed recent self-supervised learning approaches pretrained on Tobacco-1M, demonstrating the effectiveness of our architecture and training strategy. Incorporating product descriptions further improved performance, achieving 78.3% Top-1 and 83.1% Top-5 accuracy. These results affirm the Tobacco Foundation Model’s efficacy in generating rich, domain-specific representations for tobacco product classification tasks.

Visualization Results. Fig. 5 visualizes the attention maps of our model compared to MAE [18] pre-trained on the our proposed dataset. While MAE’s attention disperses across background textures, DEFEND demonstrates precise focus on discriminative features such as warning labels,

Table 3. Classification results on PHAD dataset. Here, Desc.: Description.

Method	Desc.	Pre-train Data	Acc@1 (%)	Acc@5 (%)
ResNet-50 [16]	✗	ImageNet1K	70.5	73.8
EfficientNet [38]	✗	ImageNet1K	71.4	74.7
ViT-B [13]	✗	ImageNet1K	72.5	75.6
DINO [3]	✗	Tobacco-1M	72.8	75.9
MAE [18]	✗	Tobacco-1M	73.0	76.1
CoCa [47]	✓	Tobacco-1M	73.2	76.4
DEFEND (Ours)	✗	Tobacco-1M	77.6	82.7
DEFEND (Ours)	✓	Tobacco-1M	78.3	83.1

brand identifiers, and product contours. This targeted attention mechanism directly contributes to our model’s superior classification performance, particularly in challenging scenarios with complex backgrounds or partial occlusions.



Figure 5. **Attention Visualization.** Compared to MAE [18], our model demonstrates enhanced sensitivity to product-specific details in tobacco imagery. The model effectively highlights key product features and warning labels, maintaining robust attention even in challenging scenarios with varied backgrounds and user-generated content. **Best viewed in color.**

Tobacco Products VQA Task. We evaluated DEFEND on the VQA task using the Tobacco-1M dataset, comparing it against state-of-the-art vision-language models across four question categories: Product Classification (PC), Usage Context (UC), Content Description (CD), and Health Impact (HI). All models were pre-trained on Tobacco-1M’s train set and fine-tuned for the VQA task. Results on the test set are shown in Table 4. For experimentation details, please refer to Sec. E.1 of the Supp. Our model outperforms all baselines across question categories, with notable improvements in Product Classification (+1.4%) and Usage Context (+1.5%) compared to MDETR [20]. The consistent performance across categories demonstrates DEFEND’s robust understanding of tobacco products’ visual attributes,

Table 4. Visual Question Answering results on Tobacco-1M test set across question categories

Model	Accuracy (%)					F1
	Overall	PC	UC	CD	HI	Score
ViLBERT [29]	65.3	67.8	64.2	64.5	64.7	0.67
CLIP [37]	66.9	69.2	65.8	65.9	66.7	0.68
CoCa [47]	68.4	70.8	67.5	67.2	68.1	0.70
Flamingo [1]	69.8	72.1	68.7	68.6	69.8	0.71
MiniGPT-4 [52]	71.2	73.5	70.1	70.3	70.9	0.72
MDETR [20]	72.5	74.8	71.4	71.6	72.2	0.74
DEFEND (Ours)	73.8	76.2	72.9	72.8	73.3	0.75

Note: *Overall* is the average of the given categories.

usage patterns, and health implications, making it particularly valuable for regulatory compliance and public health applications.

Zero-shot Tobacco Product Classification. We tested our DEFEND’s ability to classify novel tobacco products using the PHAD dataset as shown in Table 5. The model leverages learned representations to match unseen product images with category descriptions. This approach allows for the identification of emerging tobacco products without additional training. Our model achieved 45.6% accuracy, outperforming CLIP, CoCa, and MDETR. These results demonstrate the model’s robust generalization capabilities and potential for adapting to evolving tobacco markets and regulatory challenges.

Table 5. Zero-shot classification results on PHAD dataset.

Model	Accuracy (%)
CLIP [37]	35.8
CoCa [47]	38.4
MDETR [20]	40.9
DEFEND (Ours)	45.6

6. Conclusions

This paper introduces Tobacco-1M, a comprehensive dataset of 1M tobacco product images with hierarchical annotations, and DEFEND, a novel foundation model for tobacco product understanding. By incorporating the Feature Enhancement Module, the Local-Global Visual Coherence, and the Enhanced Image-Text Alignment mechanisms, DEFEND achieves superior performance in product classification, marketing analysis, and health impact assessment. The model’s strong zero-shot learning and visual question-answering capabilities demonstrate its effectiveness in identifying emerging tobacco products.

Limitations. While DEFEND shows promising results, it has several limitations. The model’s performance may be constrained when dealing with extremely novel tobacco

products that significantly differ from those in the Tobacco1M dataset. Its effectiveness across diverse cultural contexts and non-English packaging requires further investigation. In addition, the model’s applicability to related public health domains without extensive retraining remains unexplored. Future work should address these limitations to enhance the model’s versatility and real-world applicability in global tobacco control efforts.

References

- [1] Jean-Baptiste Alayrac, Jeff Donahue, Pauline Luc, Antoine Miech, Iain Barr, Yana Hasson, Karel Lenc, Arthur Mensch, Katherine Millican, Malcolm Reynolds, et al. Flamingo: a visual language model for few-shot learning. *Advances in neural information processing systems*, 35:23716–23736, 2022. [8](#)
- [2] Morris Alper and Hadar Averbuch-Elor. Emergent visual-semantic hierarchies in image-text representations. *arXiv preprint arXiv:2407.08521*, 2024. [2](#)
- [3] Mathilde Caron, Hugo Touvron, Ishan Misra, Hervé Jégou, Julien Mairal, Piotr Bojanowski, and Armand Joulin. Emerging properties in self-supervised vision transformers. In *ICCV*, 2021. [2](#), [8](#)
- [4] Naga VS Chappa, Pha Nguyen, Alexander H Nelson, Han-Seok Seo, Xin Li, Page Daniel Dobbs, and Khoa Luu. Sogar: Self-supervised spatiotemporal attention-based social group activity recognition. *arXiv preprint arXiv:2305.06310*, 2023. [2](#)
- [5] Naga VS Chappa, Pha Nguyen, Alexander H Nelson, Han-Seok Seo, Xin Li, Page Daniel Dobbs, and Khoa Luu. Spartan: Self-supervised spatiotemporal transformers approach to group activity recognition. In *Proceedings of the IEEE/CVF Conference on Computer Vision and Pattern Recognition*, pages 5157–5167, 2023. [2](#)
- [6] Naga VS Raviteja Chappa, Charlotte McCormick, Susana Rodriguez Gongora, Page Daniel Dobbs, and Khoa Luu. Advanced deep learning techniques for tobacco usage assessment in tiktok videos. In *2024 IEEE Green Technologies Conference (GreenTech)*, pages 162–163. IEEE, 2024. [2](#)
- [7] Naga VS Raviteja Chappa, Pha Nguyen, Page Daniel Dobbs, and Khoa Luu. React: Recognize every action everywhere all at once. *Machine Vision and Applications*, 35(4):102, 2024. [2](#)
- [8] Naga Venkata Sai Raviteja Chappa, Charlotte McCormick, Susana Rodriguez Gongora, Page Daniel Dobbs, and Khoa Luu. Public health advocacy dataset: A dataset of tobacco usage videos from social media. *TechRxiv*, 2024. [2](#), [3](#), [6](#)
- [9] Naga Venkata Sai Raviteja Chappa, Pha Nguyen, Thi Hoang Ngan Le, Page Daniel Dobbs, and Khoa Luu. Hatt-flow: Hierarchical attention-flow mechanism for group-activity scene graph generation in videos. *Sensors*, 24(11): 3372, 2024. [2](#)
- [10] Haokun Chen, Yao Zhang, Denis Krompass, Jindong Gu, and Volker Tresp. Feddat: An approach for foundation model finetuning in multi-modal heterogeneous federated learning. In *Proceedings of the AAAI Conference on Artificial Intelligence*, pages 11285–11293, 2024. [2](#)
- [11] Xinlei Chen, Haoqi Fan, Ross Girshick, and Kaiming He. Improved baselines with momentum contrastive learning. 2020. [2](#)
- [12] Jacob Devlin, Ming-Wei Chang, Kenton Lee, and Kristina Toutanova. Bert: Pre-training of deep bidirectional transformers for language understanding. *arXiv preprint arXiv:1810.04805*, 2018. [5](#), [7](#)
- [13] Alexey Dosovitskiy, Lucas Beyer, Alexander Kolesnikov, Dirk Weissenborn, Xiaohua Zhai, Thomas Unterthiner, Mostafa Dehghani, Matthias Minderer, Georg Heigold, Sylvain Gelly, et al. An image is worth 16x16 words: Transformers for image recognition at scale. *arXiv preprint arXiv:2010.11929*, 2020. [6](#), [8](#)
- [14] Haoqi Fan, Bo Xiong, Karttikeya Mangalam, Yanghao Li, Zhicheng Yan, Jitendra Malik, and Christoph Feichtenhofer. Multiscale vision transformers. *arXiv preprint arXiv:2104.11227*, 2021. [4](#)
- [15] Juan Jose Garau-Luis, Patrick Bordes, Liam Gonzalez, Masa Roller, Bernardo P de Almeida, Lorenz Hexemer, Christopher Blum, Stefan Laurent, Jan Grzegorzewski, Maren Lang, et al. Multi-modal transfer learning between biological foundation models. *arXiv preprint arXiv:2406.14150*, 2024. [2](#)
- [16] Kaiming He, Xiangyu Zhang, Shaoqing Ren, and Jian Sun. Deep residual learning for image recognition. In *Proceedings of the IEEE conference on computer vision and pattern recognition*, pages 770–778, 2016. [8](#)
- [17] Kaiming He, Haoqi Fan, Yuxin Wu, Saining Xie, and Ross Girshick. Momentum contrast for unsupervised visual representation learning. In *CVPR*, 2020. [2](#)
- [18] Kaiming He, Xinlei Chen, Saining Xie, Yanghao Li, Piotr Dollár, and Ross Girshick. Masked autoencoders are scalable vision learners. In *Proceedings of the IEEE/CVF conference on computer vision and pattern recognition*, pages 16000–16009, 2022. [4](#), [7](#), [8](#)
- [19] Chao Jia, Yinfei Yang, Ye Xia, Yi-Ting Chen, Zarana Parekh, Hieu Pham, Quoc Le, Yun-Hsuan Sung, Zhen Li, and Tom Duerig. Scaling up visual and vision-language representation learning with noisy text supervision. In *International conference on machine learning*, pages 4904–4916. PMLR, 2021. [2](#)
- [20] Aishwarya Kamath, Mannat Singh, Yann LeCun, Gabriel Synnaeve, Ishan Misra, and Nicolas Carion. Mdetrm: modulated detection for end-to-end multi-modal understanding. In *Proceedings of the IEEE/CVF international conference on computer vision*, pages 1780–1790, 2021. [8](#)
- [21] Yan Kang, Tao Fan, Hanlin Gu, Xiaojin Zhang, Lixin Fan, and Qiang Yang. Grounding foundation models through federated transfer learning: A general framework. *arXiv preprint arXiv:2311.17431*, 2023. [2](#)
- [22] Nayoung Kim, Wei-Yin Loh, and Danielle E McCarthy. Machine learning models of tobacco susceptibility and current use among adolescents from 97 countries in the global youth tobacco survey, 2013–2017. *PLOS Global Public Health*, 1(12):e0000060, 2021. [2](#)

- [23] Grace Kong, Alex Sebastian Schott, Juhan Lee, Hassan Dashtian, and Dhiraj Murthy. Understanding e-cigarette content and promotion on youtube through machine learning. *Tobacco control*, 32(6):739–746, 2023. 2
- [24] Róbert Lakatos, Péter Pollner, András Hajdu, and Tamás Joó. A multimodal deep learning architecture for smoking detection with a small data approach. *Frontiers in Artificial Intelligence*, 7:1326050, 2024. 2
- [25] Haotian Liu, Chunyuan Li, Qingyang Wu, and Yong Jae Lee. Visual instruction tuning. *Advances in neural information processing systems*, 36, 2024. 2
- [26] I Loshchilov. Decoupled weight decay regularization. *arXiv preprint arXiv:1711.05101*, 2017. 7
- [27] Ilya Loshchilov and Frank Hutter. Sgdr: Stochastic gradient descent with warm restarts. *arXiv preprint arXiv:1608.03983*, 2016. 7
- [28] Cewu Lu, Ranjay Krishna, Michael Bernstein, and Li Fei-Fei. Visual relationship detection with language priors. In *Proceedings of the European Conference on Computer Vision (ECCV)*, pages 852–869, 2016. 2
- [29] Jiasen Lu, Dhruv Batra, Devi Parikh, and Stefan Lee. Vilbert: Pretraining task-agnostic visiolinguistic representations for vision-and-language tasks. *Advances in neural information processing systems*, 32, 2019. 8
- [30] Yizhen Luo, Kai Yang, Massimo Hong, Xing Yi Liu, and Zaiqing Nie. Molfm: A multimodal molecular foundation model. *arXiv preprint arXiv:2307.09484*, 2023. 2
- [31] Andriy Mnih and Geoffrey E Hinton. A scalable hierarchical distributed language model. *Advances in neural information processing systems*, 21, 2008. 2
- [32] Dhiraj Murthy, Juhan Lee, Hassan Dashtian, Grace Kong, et al. Influence of user profile attributes on e-cigarette-related searches on youtube: Machine learning clustering and classification. *JMIR infodemiology*, 3(1):e42218, 2023. 2
- [33] Dhiraj Murthy, Rachel R Ouellette, Tanvi Anand, Sriyith Radhakrishnan, Nikhil C Mohan, Juhan Lee, and Grace Kong. Using Computer Vision to Detect E-cigarette Content in TikTok Videos. *Nicotine & Tobacco Research*, 26 (Supplement_1):S36–S42, 2024. 2, 3
- [34] Hoang-Quan Nguyen, Thanh-Dat Truong, Xuan Bac Nguyen, Ashley Dowling, Xin Li, and Khoa Luu. Insect-foundation: A foundation model and large-scale 1m dataset for visual insect understanding. In *Proceedings of the IEEE/CVF Conference on Computer Vision and Pattern Recognition*, pages 21945–21955, 2024. 3
- [35] Pha Nguyen, Kha Gia Quach, Kris Kitani, and Khoa Luu. Type-to-track: Retrieve any object via prompt-based tracking. *Advances in Neural Information Processing Systems*, 36, 2024. 2
- [36] Olga Perski, Kezhi Li, Nikolas Pontikos, David Simons, Stephanie P Goldstein, Felix Naughton, and Jamie Brown. Classification of lapses in smokers attempting to stop: A supervised machine learning approach using data from a popular smoking cessation smartphone app. *Nicotine and Tobacco Research*, 25(7):1330–1339, 2023. 2
- [37] Alec Radford, Jong Wook Kim, Chris Hallacy, Aditya Ramesh, Gabriel Goh, Sandhini Agarwal, Girish Sastry, Amanda Askell, Pamela Mishkin, Jack Clark, et al. Learning transferable visual models from natural language supervision. In *International conference on machine learning*, pages 8748–8763. PMLR, 2021. 2, 4, 6, 8
- [38] Mingxing Tan and Quoc Le. Efficientnet: Rethinking model scaling for convolutional neural networks. In *International conference on machine learning*, pages 6105–6114. PMLR, 2019. 8
- [39] Kaihua Tang, Hanwang Zhang, Baoyuan Wu, Wenhan Luo, and Wei Liu. Learning to compose dynamic tree structures for visual contexts. In *Proceedings of the IEEE/CVF conference on computer vision and pattern recognition*, pages 6619–6628, 2019. 2
- [40] Julia Vassey, Chris J Kennedy, Ho-Chun Herbert Chang, Ashley S Smith, and Jennifer B Unger. Scalable Surveillance of E-Cigarette Products on Instagram and TikTok Using Computer Vision. *Nicotine & Tobacco Research*, 26(5): 552–560, 2023. 2, 3
- [41] Chien-Yao Wang, Alexey Bochkovskiy, and Hong-Yuan Mark Liao. Yolov7: Trainable bag-of-freebies sets new state-of-the-art for real-time object detectors. In *Proceedings of the IEEE/CVF conference on computer vision and pattern recognition*, pages 7464–7475, 2023. 2
- [42] Mengmeng Wang, Jiazheng Xing, and Yong Liu. Actionclip: A new paradigm for video action recognition. *arXiv preprint arXiv:2109.08472*, 2021. 2
- [43] Xiaoping Wu, Chi Zhan, Yu-Kun Lai, Ming-Ming Cheng, and Jufeng Yang. Ip102: A large-scale benchmark dataset for insect pest recognition. In *Proceedings of the IEEE/CVF conference on computer vision and pattern recognition*, pages 8787–8796, 2019. 2, 3
- [44] Haiyang Xu, Qinghao Ye, Ming Yan, Yaya Shi, Jiabo Ye, Yuanhong Xu, Chenliang Li, Bin Bi, Qi Qian, Wei Wang, et al. mplug-2: A modularized multi-modal foundation model across text, image and video. In *International Conference on Machine Learning*, pages 38728–38748. PMLR, 2023. 2
- [45] Haohang Xu, Xiaopeng Zhang, Hao Li, Lingxi Xie, Wenrui Dai, Hongkai Xiong, and Qi Tian. Seed the views: Hierarchical semantic alignment for contrastive representation learning. *IEEE Transactions on Pattern Analysis and Machine Intelligence*, 45(3):3753–3767, 2023. 4
- [46] Keren Ye and Adriana Kovashka. Linguistic structures as weak supervision for visual scene graph generation. In *Proceedings of the IEEE/CVF Conference on Computer Vision and Pattern Recognition*, pages 8289–8299, 2021. 2
- [47] Jiahui Yu, Zirui Wang, Vijay Vasudevan, Legg Yeung, Mojtaba Seyedhosseini, and Yonghui Wu. Coca: Contrastive captioners are image-text foundation models. *arXiv preprint arXiv:2205.01917*, 2022. 4, 6, 8
- [48] Alireza Zareian, Svebor Karaman, and Shih-Fu Chang. Bridging knowledge graphs to generate scene graphs. In *Computer Vision—ECCV 2020: 16th European Conference, Glasgow, UK, August 23–28, 2020, Proceedings, Part XXIII 16*, pages 606–623. Springer, 2020. 2
- [49] Alireza Zareian, Zhecan Wang, Haoxuan You, and Shih-Fu Chang. Learning visual commonsense for robust scene graph

- generation. In *Computer Vision–ECCV 2020: 16th European Conference, Glasgow, UK, August 23–28, 2020, Proceedings, Part XXIII 16*, pages 642–657. Springer, 2020.
- [50] Howard Zhong, Samarth Mishra, Donghyun Kim, SouY-oung Jin, Rameswar Panda, Hilde Kuehne, Leonid Karlinsky, Venkatesh Saligrama, Aude Oliva, and Rogerio Feris. Learning human action recognition representations without real humans. *Advances in Neural Information Processing Systems*, 36, 2024.
- [51] Yiwu Zhong, Jing Shi, Jianwei Yang, Chenliang Xu, and Yin Li. Learning to generate scene graph from natural language supervision. In *Proceedings of the IEEE/CVF International Conference on Computer Vision*, pages 1823–1834, 2021. 2
- [52] Deyao Zhu, Jun Chen, Xiaoqian Shen, Xiang Li, and Mohamed Elhoseiny. MiniGPT-4: Enhancing vision-language understanding with advanced large language models. In *The Twelfth International Conference on Learning Representations*, 2024. 8